Structures 60 (2024) 105968

Contents lists available at ScienceDirect

Structures

journal homepage: www.elsevier.com/locate/structures

Analytical prediction of load-deformation behaviour for bearing at bolt holes

Primož Može *, Sara Piculin

University of Ljubljana, Faculty of Civil and Geodetic Engineering, Jamova cesta 2, 1000 Ljubljana, Slovenia

A R T I C L E I N F O

Keywords:
Bearing
Bolt hole
Bolted connection
Bolted joint
Component method
Eurocode
EN 1993–1-8

A B S T R A C T

Although bolted bearing-type connections are widely used in steel structures, knowledge of their deformation behaviour is limited. Deformation behaviour is particularly important for nominally pinned connections, lap connections and other connections with bolts in bearing. Bolted bearing-type connections are characterised by non-linear deformation behaviour in terms of yielding of the material in front of the bolt hole, which occurs at the beginning of the deformation path due to the embedding of the bolt in the steel plate. The paper deals with the formulation of a non-linear analytical expression that describes the embedding of the bolt and allows the designer to estimate the deformation of the bolt hole due to the bearing. The expression was derived based on numerical analysis and confirmed by tests on bolted lap connections made of mild and high-strength steels. Test results of lap joints with different geometries, number of bolts, steel grades and failure modes are also used to demonstrate the applicability of the prediction model. Comparison to the existing Eurocode linear load-deformation model for bearing is also shown. It is shown that the load-deformation relationship for bearing at bolt holes proposed in this paper, which is already included in the new generation of the Eurocode for the design of joints in steel structures, can predict the load-deformation behaviour well. The bearing resistance limit to control the bearing deformation and a simplified linear load-deformation model based on the proposed non-linear model are also presented.

1. Introduction

Bolts are normally used in clearance holes, where the clearance allows for fabrication tolerances and simplifies the fabrication and assembly of the connections. In bearing type connections, where the forces are transmitted through the contact between the bolt and the wall of bolt hole, the distribution of forces between all the bolts in the connection is achieved by the ductility of the steel, which allows the bolt to be embedded. The embedding of the bolt is crucial to achieve a uniform distribution of forces between the bolts, which contributes to a uniform utilization of the bolts in shear and thus to simple design rules. Fig. 1 shows a lap joint with 4 bolts, its mechanical model and the distribution of forces between the bolts. The mechanical spring model is usually used to determine the distribution of forces between bolts [1,2]. The spring S_t represents the plate between the bolts in tension, while the equivalent springs S_b represents the bolt in shear and the plate in bearing. The uneven distribution of forces between bolts arises from the compatibility of deformations between two bolts [2,3]. It typically occurs when the elongations of the two springs S_t and S_b are the same order of magnitude. The distribution of forces uniforms when the deformation of spring S_b is much greater than that of spring S_t, which is possible due to different stiffness of the springs. Uneven distribution is characteristic for long connections, for connections with large bolt spacing and for connections with highly stressed plates, which is relevant for HSS where the elastic elongations can be quite large. The plate in bearing is related to the embedment of the bolt, which leads to elongation of the bolt hole. The elongation of the bolt hole can be several orders of magnitude greater than the elongation of the plate in tension. Therefore, a uniform distribution can be assumed as soon as embedding of the bolt is activated. However, the bolts should have sufficient strength to withstand the bearing forces generated during embedment. Otherwise, the distribution of forces between bolts will remain uneven because the bolt holes cannot deform. Therefore, even in short connections, there may be an uneven distribution of forces between the bolts if the bolts are weak. For this reason, it is important to understand the behaviour of the bearing at the bolt holes.

The component method given in the Eurocode for the design of joints in steel structures EN 1993–1-8 [4] provides two models (linear and

* Corresponding author.
E-mail address: primoz.moze@fgg.uni-lj.si (P. Može).

https://doi.org/10.1016/j.istruc.2024.105968
Received 22 May 2023; Received in revised form 1 December 2023; Accepted 24 January 2024
Available online 1 February 2024
2352-0124/© 2024 The Author(s). Published by Elsevier Ltd on behalf of Institution of Structural Engineers. This is an open access article under the CC BY license (http://creativecommons.org/licenses/by/4.0/).

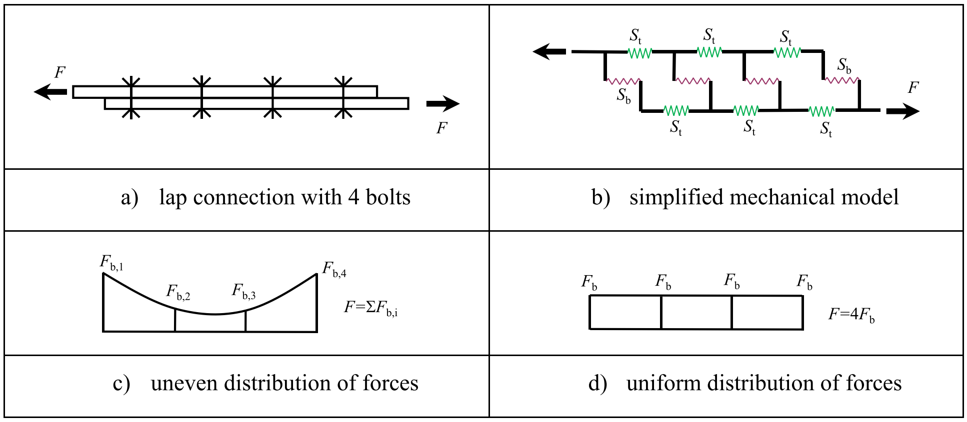

Fig. 1. Schemes of lap connection and the possible distribution of forces between bolts.

non-linear) for predicting the load-deformation behaviour for bearing at bolt holes. Both models can be used with newly defined bearing resistance, which is easier to apply and provides higher resistance. The characteristic value of the bearing resistance is given by:

$$F_b = k_m \alpha_b \, d \, t f_u \tag{1}$$

$$\alpha_b = \begin{cases} \min\left(\frac{e_1}{d_0};\ 3\frac{f_{ub}}{f_u};\ 3\right) & \text{for end bolt} \\ \min\left(\frac{p_1}{d_0}-\frac{1}{2};\ 3\frac{f_{ub}}{f_u};\ 3\right) & \text{for inner bolt} \end{cases} \tag{2}$$

$$k_m = \begin{cases} 0.9; & \text{for steel grades} \geq \text{S460} \\ 1; & \text{otherwise} \end{cases} \tag{3}$$

where d is the bolt diameter, d_0 is the diameter of the normal round bolt hole, t is the plate thickness, f_u is the ultimate strength of the plate, f_{ub} is the ultimate strength of bolt, e_1 is the plate end distance and p_1 is the spacing between centers of bolt holes. The designations correspond to the Eurocode.

The first model for predicting the load-deformation behaviour for bearing, already included in the first generation of the Eurocode [5], provides an elastic stiffness that depends on the position of the bolt in relation to the edges and other bolts. This model is used to predict the yield deformation and is not able to accurately describe the bolt embedment. The elastic stiffness for bearing for a single bolt hole is given by:

$$k_b = 12 \ k_d \, k_t \, d \, f_u \tag{4}$$

$$k_d = \min\left(\frac{e_1}{4\cdot d}+\frac{1}{2};\quad 0.25\frac{p_1}{4\cdot d}+\frac{3}{8};\quad 1.25\right) \tag{5}$$

$$k_t = \min\left(1.5\frac{t}{d_{M16}};\quad 2.5\right) \tag{6}$$

where d_{M16} is nominal diameter of an M16 bolt. Eurocode provides the stiffness coefficient for a bolt row, where a bolt row has two bolts. Therefore, the coefficient in Eq. (4) is 12 and not 24 as in the Eurocode.

The second model proposed by the corresponding author and presented in this paper describes the embedment of the bolt and is described in detail in Section 3. Although the load deformation model for bearing presented in this paper has been included in the new Eurocode [4] and has already been discussed in the literature [6,7], the full background information on the model has not yet been published.

Important investigations into the distribution of forces in splice joints were carried out by Fisher and Rumpf [1]. Based on experimental results, they developed analytical expressions to describe the load-deformation relationships of bolts in shear and plate in bearing. They showed it is a non-linear relationship described by a logarithmic function specific to each test. A disadvantage of this model is that it cannot be generalized and that the two components, bolt in shear and plate in bearing, cannot be separated. Rex and Easterling [8] recognised that the relative load-deformation behaviour for bearing is the simplest way to represent the behaviour and gave some guidance on how to construct the load-deformation curve. Može [9,10] showed that the load-deformation curves have clear trends and similarities when presented in the relative form. Yi-Fan Lyu et al. [11] have identified three stages of the bearing process. Stage I refers to the formation of the initial contact when only a limited part of the material around the bolt hole yields and the elongation of the bolt hole is negligible. Resistance develops at stage II, when most of the plate material in front of the bolt hole yields, but no significant change of slope of the load-displacement curve is observed. At the end of stage II, about 88% of the ultimate bearing resistance is reached, while 32% of the bolt hole elongation has accumulated. Stage III is characterized by plastic behaviour, where the remaining 12% of the resistance is gained while the remaining 68% of bolt hole elongation is accumulated. Ahmed and Teh [12] showed that the end and edge distances do not have a significant effect on the elastic stiffness, but the plates with fully threaded bolts appear to have a lower initial stiffness than the comparable shank specimens. They showed that the effects of the threads were more pronounced for thin plates of 4.7 mm than for plates of 8 mm thickness. As mentioned, the load-deformation model for bearing presented in this paper has already been discussed in the literature. It was tested on lap connections with threads in one plate [7]. It was concluded that the codified load-deformation relationship is correctly determined for standard assemblies (bolt with nut), while a reduction of about 15% is required for connections with threads in one plate (only bolt without nut). The validation and application of the new load-deformation relationship for bearing is shown in [6] for bolted connections with a specific geometry and bolt arrangement that require high local ductility to achieve the predicted resistances according to [4]. It has been shown that load-deformation relationship for bearing given in the new Eurocode [4] agrees well with experimental and numerical results.

The aim of this paper is to propose an analytical model for bearing load-deformation behaviour and validate this model with test results. The analytical model for bearing is important when dealing with simplified mechanical models that can be used to determine, for example, the distribution of forces between bolts and the associated design rules for lap joints, the effect of lap joints on the deformation of the whole structure, the ductility demands for nominally pinned joints, etc. The mechanical behaviour is explained in detail and supported by numerical analyses. The analytical prediction of the load-deformation relationship for bearing is compared to the experimental results of connections with only one bolt and with the results of connections with several bolts where different failure modes were observed.

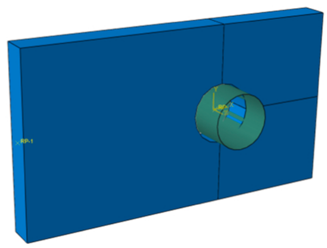

Fig. 2. Presentation of numerical model.

Table 1
Abaqus input of material plasticity.

True stress [MPa]	313	423.5	508.4	700
Plastic strain	0	0.047	0.18	0.68

2. Finite element analysis

The deformation behaviour of the steel plate in the bolt bearing is a problem of contact mechanics. Analytical solutions found in the literature exist mainly for elastic contacts between different bodies. Bolted shear connections between steel elements are characterized by local yielding of the plate at the bolt hole, which makes bolted connections an efficient technique of joining and simplifies the design rules. The deformation behaviour for bearing at bolt holes is described using finite element analysis (FEA) of a single bolt connection, which shows the relationships between different parameters. The FEA results provide insight into the bearing behaviour and justify the adoption of the analytical load-deformation relationship (Chapter 3), which is applied in Chapter 4 to single-bolt lap connections and multiple-bolt lap connections that failed in different failure modes.

2.1. Numerical modeling

Finite element analysis was used to understand the deformation behaviour of steel plates in bearing at bolt holes. The numerical models and geometry of the connections are presented in detail in [9,13]. Only a brief summary is presented in this paper. A relatively simple numerical model was created in the finite element software Abaqus to represent single bolt connections. The model shown in Fig. 2 consists of a deformable steel plate and a rigid tube representing the bolt. A "hard" contact relationship was defined between the two bodies. The model was meshed with linear bricks with eight nodes and incompatible modes (C3D8I) that maintain a constant volume during plastic deformation, but C3D8I did not achieve convergence at large hole elongations. In addition, linear triangular prisms with 6 nodes (C3D6) were used to complete the mesh. The size of the finite elements was about 2.5 mm, with 6 elements considered over the plate thickness. The structural steel was modelled as an elastic–plastic material. The elastic behaviour was defined by the Young's modulus and Poisson's ratio, which are equal to $E = 210000$ MPa and $\nu = 0.3$. The Mises yield surface was used to define isotropic yielding. The true stresses and strains for S235 steel were determined by numerical simulation of the standard tensile test to which the material model was calibrated [9]. The data is given in Table 1 while additional information can be found in [9]. A simple numerical model was chosen because of its efficiency. A model with bolt and lap plates gives similar results. The comparison between these models can be found in [9,13].

To demonstrate of the behaviour of bearing at bolt holes, the assembly of a 27 mm diameter tube (representing the bolt) and 10, 30 and 50 mm thick and 450 mm wide plates with a bolt hole diameter of $d_0 = 30$ mm, positioned $e_1 = 1.5d_0$, $3d_0$, $5d_0$ from the end edge was analysed. In [9] it was shown that the edge distance e_2 has no significant influence on the response as long as the plate is wide enough to prevent the net cross-section failure, so that the failure occurs due to bearing at bolt hole (shear or splitting failure). When the edge distance e_2 was increased by a factor of 4, only a 10% increase in the load-bearing resistance was observed. The bearing resistance is therefore practically independent of the edge distance e_2. Therefore, the width of the plate

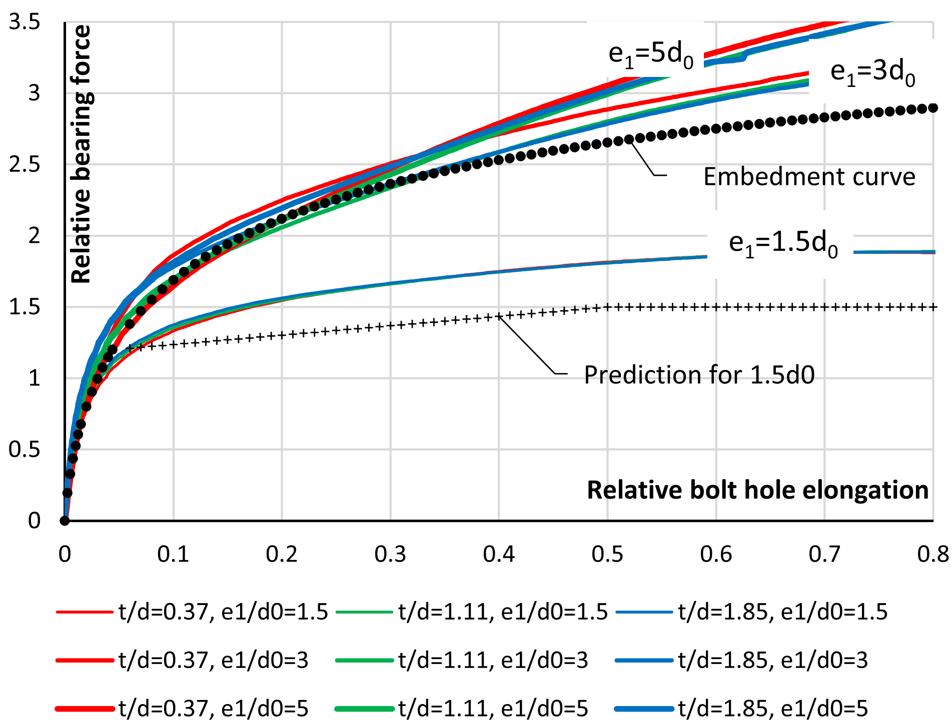

Fig. 3. Load-deformation curves for different ratios t/d and end distance $e_1 = 1.5\ d_0$, $3\ d_0$ and $5\ d_0$.

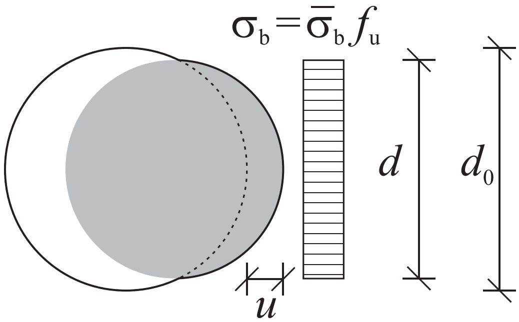

Fig. 4. Presentation of hole elongation and average bearing stress.

was kept constant.

3. Definition of load-deformation model for bearing based on the results of FEA

3.1. Findings from finite element analysis

The FEA response curves are shown in Fig. 3 in terms of relative (non-dimensional) bearing stress and relative (non-dimensional) bolt hole elongation. Several researchers have showed that when the load-deformation behaviour for bearing is represented in the relative form, the (in)dependence of various parameters can be observed [9,10,14]. Therefore, the relative form is suitable to directly compare the effects of plate thicknesses, edge distances, bolt diameters or steel grades. The relative bolt hole elongation $\bar{u}$ is represented as the bolt hole elongation u (see Fig. 4) divided by the bolt diameter d. The bearing force is represented as relative average bearing stress (or force) $\bar{\sigma}_b$, obtained by dividing the bearing force F_b by the product of the tensile strength of the plate material f_u, the plate thickness t and the bolt diameter d:

$$\bar{\sigma}_b = \frac{F_b}{d\,t\,f_u} \tag{7}$$

$$\bar{u} = \frac{u}{d} \tag{8}$$

In Fig. 3 you can see three sets of curves representing the response of connections with end distances of $e_1 = 1.5\ d_0$, $3\ d_0$ and $5\ d_0$. Each set of curves in a different colour, but with the same thickness, represents connections with the same end distance but a different ratio of thickness to bolt diameter (10/27, 30/27 and 50/27). It can be observed that the response of connections with the same end distance is similar and practically independent of the t/d ratio. Moreover, the global response is also similar for the $3\ d_0$ and $5\ d_0$ end distances. It seems that the global response is similar as soon as the end distance is large enough. Furthermore, initially all curves in Fig. 3 follow the same trend, when at some point the slope of the curves of connections with end distance 1.5 d_0 decreases faster. Figs. 5 and 6 serve to explain the global response. The figures show the equivalent plastic strain at different resistance states in plates with end distance of 1.5 d_0 and 3 d_0. Since steel is a relatively stiff material, the peaks of the contact stresses already reach the yield stress at relatively low loads (Figs. 5a, 6a). Yielding reduces the stiffness of the material, eliminates stress concentrations and allows the bolt to be embedded on a larger contact area [3]. The embedding of the bolt is related to the local yielding of the plate material and causes the deformation of the bolt hole. As the load increases, the local yielding progresses until it reaches the plate edge or the downstream bolt hole. If the end distance or bolt spacing is small, the downstream material yields at a smaller hole elongation (Fig. 5b-c), while a larger end distance or bolt spacing allows a larger bolt hole elongation, so that all the downstream material yields (Fig. 6b-d). At this stage, the bolt embeds and the stiffness gradually decreases. Although the deformation of the bolt hole is not reversible, the behaviour associated with the embedding of the bolt is interpreted as nominally elastic. Due to strain hardening, the bearing resistance increases after all downstream material has yielded, but the stiffness further decreases (Fig. 5e-f, Fig. 6e-f). At small end spacings, a plastic plateau typically develops, while at large end distance the resistance increases until fracture [13]. With the development of measuring equipment devices that allow the measurement of the displacement field and the calculation of the strains based on digital image correlation, the described mechanical behaviour could be

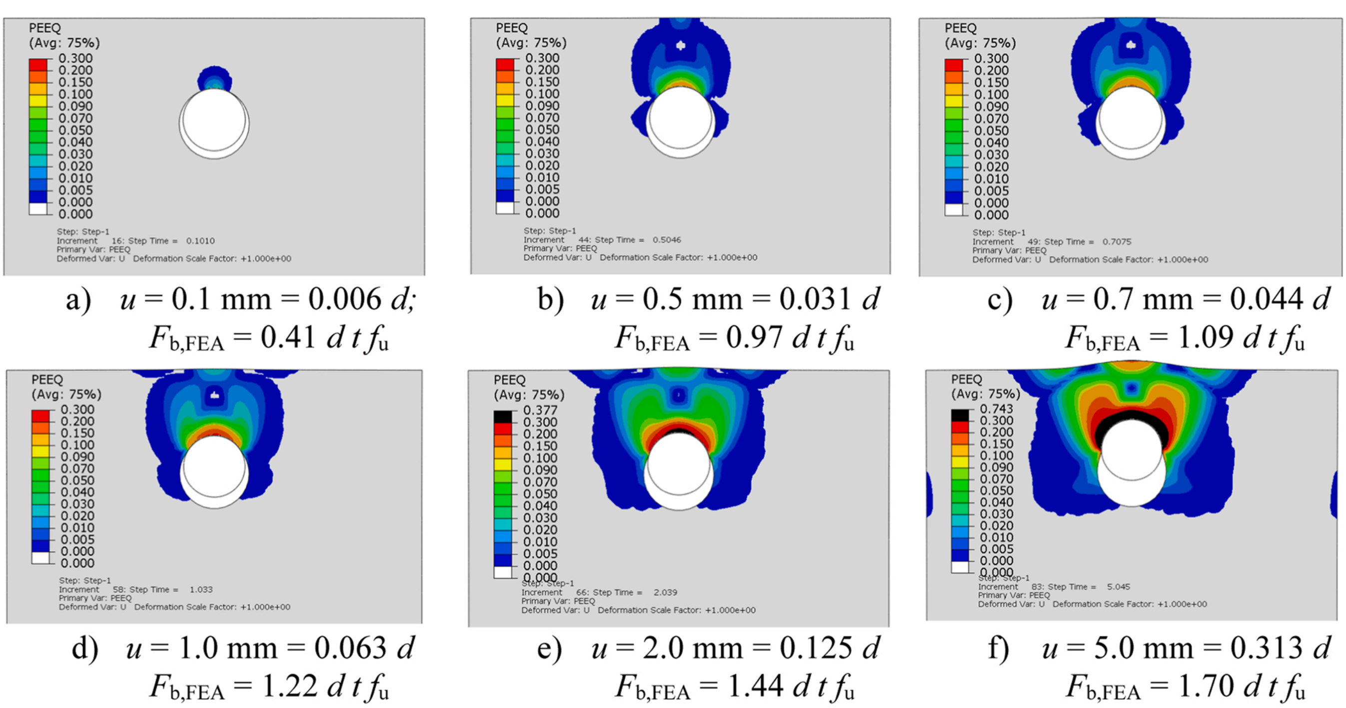

Fig. 5. Equivalent plastic strain in plate with M16 pin, steel grade S235, plate thickness $t = 8$ mm, end distance $e_1 = 1.5\ d_0$.

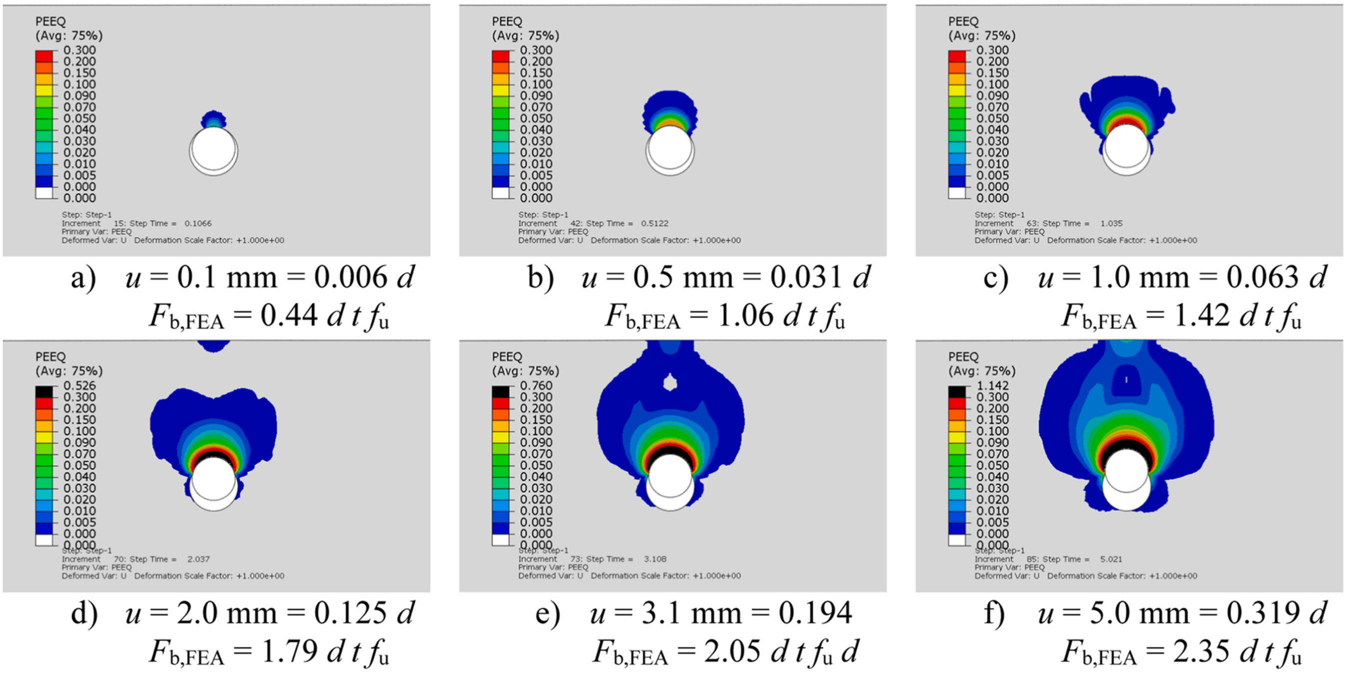

Fig. 6. Equivalent plastic strain in plate with M16 pin, steel grade S235, plate thickness $t = 8$ mm, end distance $e_1 = 3\ d_0$.

Table 2
Characteristic points of the embedment curve represented by Eq. (9).

Relative bolt hole elongation	0.009	0.030	0.044	0.074	0.165	0.320	0.380	0.545	1.00
Relative bearing stress	0.5	1.0	1.2	1.5	2.0	2.4	2.5	2.7	3.0

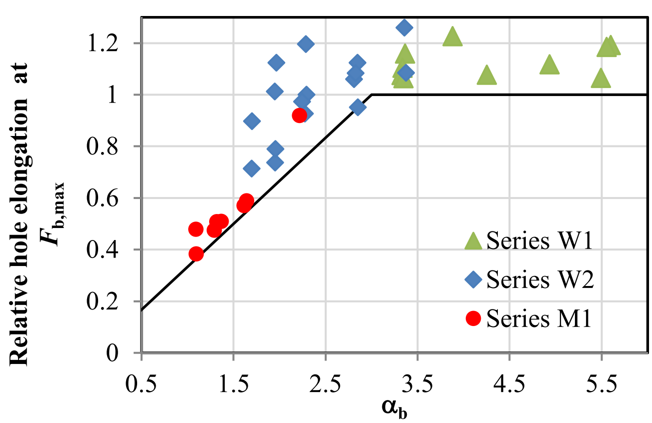

Fig. 7. Relative bolt hole elongation at maximum bearing resistance for S235 steel; M1, W1 single bolt connections in double shear, W2 connections with 2 bolts in double shear; see [9] for M1 and [13] for W1, W2.

experimentally verified [15].

3.2. Load-deformation model for bearing

The bearing deformation behaviour described in 3.1 is non-linear, with no actual elastic behaviour. The main reason for non-linearity is the embedding of the bolt, which causes a local yielding in the plate downstream of the bolt hole. Therefore, the embedding of the bolt does not depend on the distances of the bolt hole from the edges. It is also assumed (and proved in the next chapter) that the steel grade (mild structural steel or high strength structural steel) has no significant influence on the embedding of the bolt, when the load-deformation behaviour is presented in the non-dimensional form. Therefore, the embedding of the bolt can be described by the non-dimensional embedment curve as follows:

$$\overline{\sigma}_b = \frac{126\ \overline{u}}{\left(1 + \sqrt{30\,\overline{u}}\right)^2} \tag{9}$$

For ease of interpretation, the characteristic points of Eq. (9) are listed in Table 2. Fig. 3 shows that the embedment curve describes well the overall response curve obtained by FEA for a large end distance. For short end distance, the embedment was carried out up to about 80% of the maximum bearing resistance. This was also observed in [9]. The increase of the bearing resistance from 80% of the maximum resistance to the ultimate bearing resistance, which occurs at the bolt hole elongation u_u, is described by a linear dependence. When the maximum bearing resistance is reached, the yield plateau extends to the fracture (see curve “Prediction for 1.5 d_0” in Fig. 3). The displacement at ultimate resistance u_u can be determined from the test results. Fig. 7 shows the relative bolt hole elongation at maximum resistance u_u for the author’s test results for one and two bolt connections of S235 steel against α_b given by Eq. (2). The M1 series (see [9]) and W1 series (see [13]) are connections with one bolt in double shear, while the W2 series (see [13]) are connections with two bolts arranged in the direction of the bearing force. For the W2 connections, the minimum coefficient α_b for end and inner bolts is considered. The failures of all connections shown in Fig. 7 are related to the bearing at the bolt hole, i.e. shear failure or splitting failure. The solid line represents the lower limit of the hole elongation at ultimate resistance, which can be expressed as follows:

$$u_u = \min\left(\frac{\alpha_b}{3};\ 1\right)\cdot d. \tag{10}$$

The described constitution of the analytical relationship for bearing for steel grades up to S460 is shown in Fig. 8a. The maximum relative

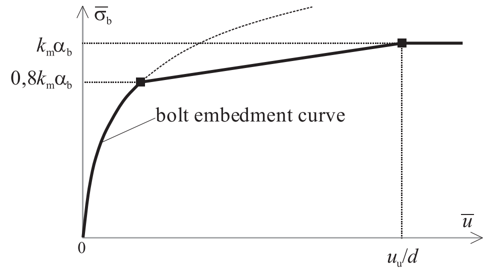

a) steels up to S460 ($k_m = 1$)

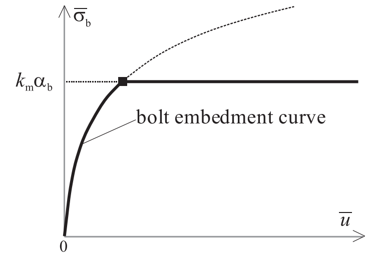

b) steels S460 and greater ($k_m = 0.9$)

Fig. 8. Presentation of analytical model for bearing.

bearing force of 3 f_u d t according to Eq. (1) is reached at a relative bolt hole elongation of 1, which agrees with the data from Eq. (9) and Eq. (10). For end distances $e_1 \geq 3\ d_0$ or bolt spacings $p_1 \geq 3.5\ d_0$ ($\alpha_b = 3$), only the embedment curve Eq. (9) can be used to describe both the embedding and the plastic phase (in two stages), while for smaller distances ($\alpha_b < 3$) the analytical response curve must be constructed in three stages, as shown in Fig. 8a and described above.

Different steel grades influence the bearing behaviour during the transition from the bolt embedment stage (nominally elastic) to the plastic stage. The differences in the bearing behaviour of mild S235 and high-strength S690 steel are shown in [9]. HSS are characterized by a sharper transition from nominally elastic to plastic behaviour and show that the plastic behaviour is characterized by a slightly decreasing plastic plateau. The bearing resistance of HSS is reduced by the material factor k_m, equalling 0.9 for steel grade greater and including S460 (see Eq. (3)). The factor k_m indirectly considers the ductility requirements related to the bearing resistance of a group of bolts, which is calculated as the sum of the bearing resistances of the individual bolts. For this reason, the constitution of the analytical model must be adapted for HSS. The analytical model can be presented in two stages, as shown in Fig. 8b. The embedment curve given by Eq. (9) extends up to the maximum resistance, which for HSS is limited to the product of k_m α_b. The embedment curve is continued by the plastic plateau.

4. Verification of the load-deformation model for bearing by test results

The analytical load-deformation model for bearing is verified by the test results of lap connections with one and several bolts made of different types of steel. The tests used to verify of the model show extreme bolt hole elongations that are several orders of magnitude larger than the elastic deformations of the plate, which can therefore be neglected. This assumption simplifies the comparison with the test results of connections shown below, as the displacements measured in the tests include the deformation of the plate. For lap joints, the relative displacement between the plates is usually measured. This assumption also simplifies the constitution of load-deformation curves for connections with several bolts. The mechanical model of a lap joint is shown in Fig. 1b. Since the deformations of the springs S_t are several orders of magnitude smaller than those of the springs S_b, it can be assumed that they are infinitely rigid. The mechanical model of the lap joint simplifies to the model, where the springs S_b are connected in sequence. Therefore, the deformation of all springs S_b is equal.

The tests on lap connections are normally carried out to investigate the overall behaviour. Therefore, the load-deformation curves of the test results shown below are characterized by initial slip, which is clearly visible in the test curves. In addition, the contacts between the bolts and the bolt holes are usually not established simultaneously due to the geometric tolerances during manufacturing. This is noticeable by an increase in the slope of the load-deformation curve and can be seen in the curves shown below. As these effects are not taken into account in the mechanical model, some of the test curves have been moved to the left for easier comparison with the prediction curves.

4.1. Connections with single bolt

Figs. 9 to 14 show the load-deformation curves for single-bolt connections with different end distances, edge distances, steel grades, bolt diameters and the curves predicted by the linear and non-linear analytical models. Detailed information on the connections can be found in [9,13,16,17], while the information required for the determination of the analytical load-deformation curves can be found in Table 3. The failure modes of all the connections shown in the figures were related to the bearing at the bolt holes. The lap plates of the connections were thicker than the inner plates, therefore the deformations were observed in the inner plate at bolt hole. The shear deformation of the bolts was also negligible compared to the deformation due to the bearing action [9,13,16,17]. Therefore, the deformations of the lap plates and

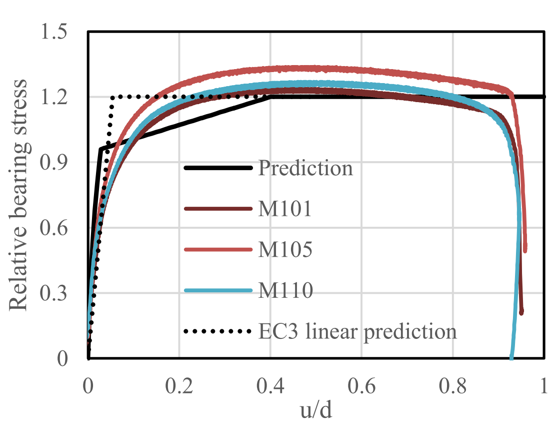

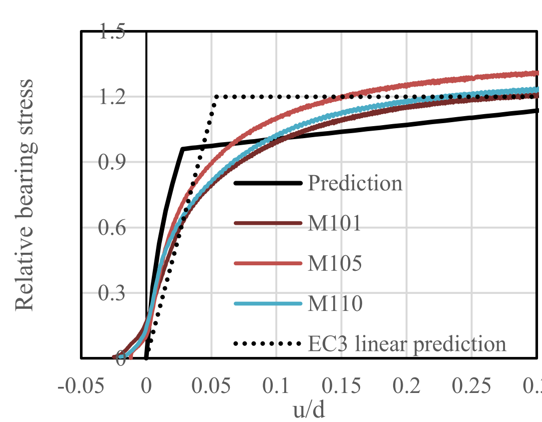

Fig. 9. Comparison of test results M101 (e_1 =1.19d_0), M105 (e_1 =1.26d_0), M110 (e_1 =1.17d_0) with the prediction curve for e_1 = 1.2d_0, steel S235, see [9].

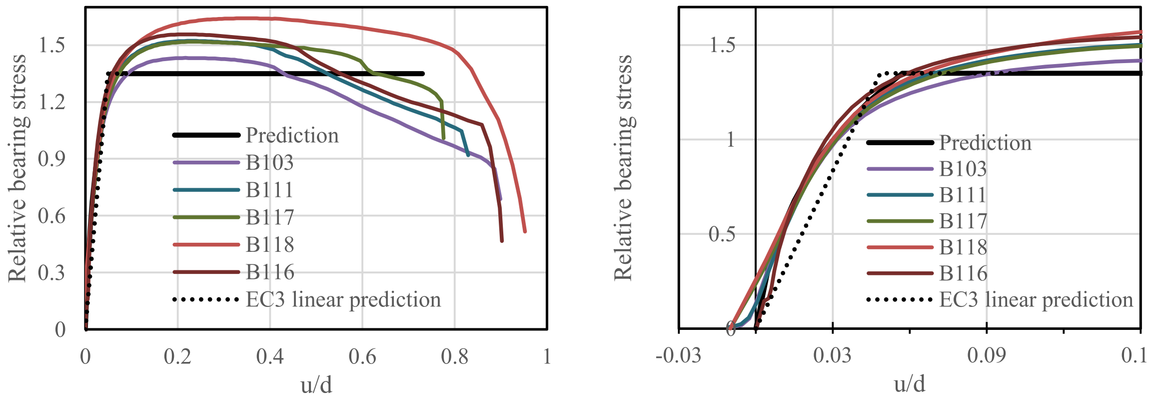

Fig. 10. Comparison of test results (series B, [16]) with the prediction curve, $e_1 = 1.5d_0$, steel S690.

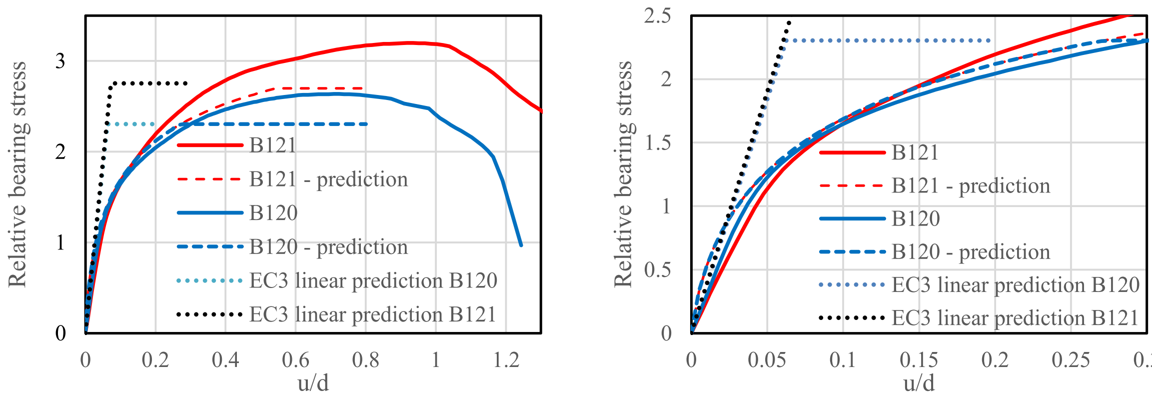

Fig. 11. Comparison of test results (series B, [16]) with the prediction curve, $e_1 = 2.56d_0$ and $e_1 = 3.06d_0$, steel S690.

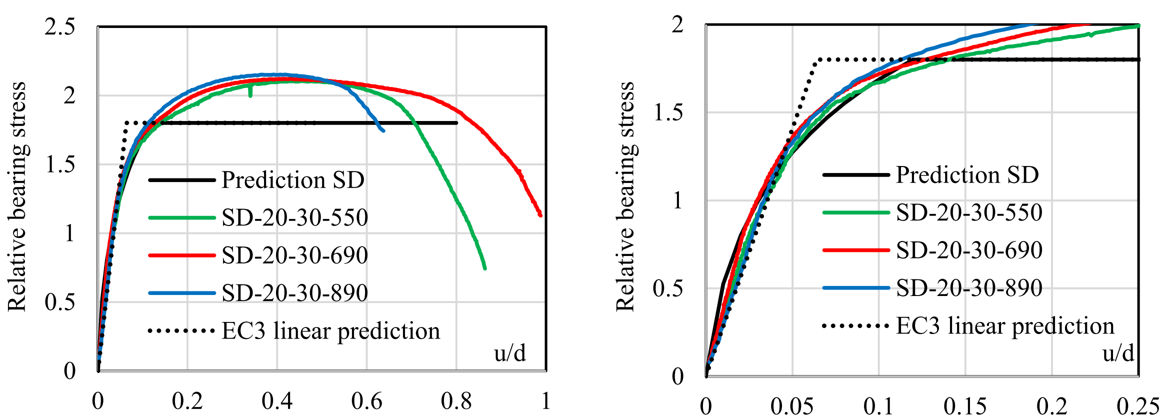

Fig. 12. Comparison of test results (series SD, [17]) with the prediction curve, $e_1 = 2d_0$, steels Q550D, Q690D, Q890D.

the deformation of the bolt can be neglected in the constitution of the prediction curves. The figures on the left show the load-deformation behaviour until failure, while the figures on the right show the embedment phase and the transition to the plastic phase. It can be concluded that the prediction model generally describes the test results well.

Fig. 9 shows that the prediction model slightly overestimates the slope of embedment curve for small end distances $e_1 = 1.2\ d_0$ for mild steel. Figs. 10 and 11 show the load-deformation curves for the high strength steel S690. It can be observed that the embedment curve fits well in the case of the end distance $e_1 = 1.5\ d_0$ to $3\ d_0$. Fig. 10 shows sharp transition from the embedment curve to the plastic plateau and the slightly negative slope of the experimental response curves in the plastic phase, which is considered by the k_m factor. The embedment curve fits almost perfectly for specimen B120, while specimen B121 shows greater deformation and resistance than the prediction curve. Specimen B121 fractured in the shear plate by splitting failure and simultaneously in the net cross-section (see [16]). Therefore, the displacement of about 0.2 d is due to the deformation of the net cross-section. In addition to the authors' own results, Fig. 12 shows the load-deformation curves of single-bolt connections with three different HSS by Wang et al. [17]. The main difference between the test curves of steel grades equivalent to S550Q, S690Q and S890Q is the deformation capacity, which decreases as the steel grade increases, while the embedment curve agrees well with the test curves.

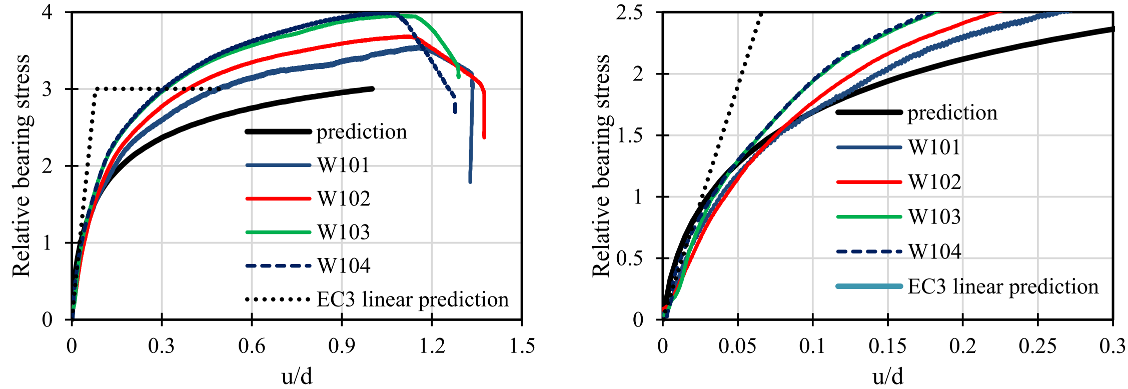

Fig. 13. Comparison of test results (series W, [13]) with the prediction curve, $e_1 = 3d_0$, steel S235.

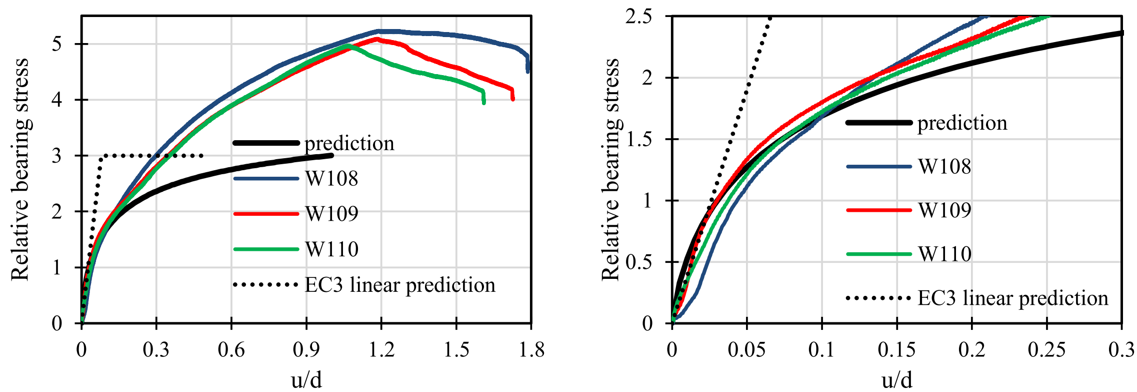

Fig. 14. Comparison of test results (series W, [13]) with the prediction curve, $e_1 = 5d_0$, steel S235.

The embedment curve describes the behaviour of connections with large end distances (3 d_0 and 5 d_0) for mild steel very well, as shown in Figs. 13 and 14. However, the resistance is clearly underestimated. Fig. 13 shows the curves of specimens W101 to W104, where the end distances are similar (3 d_0) while the width of the plate is different. The resistance increases by about 14% with the increase of the edge distance from 2.5 d_0 (W101) to 4 d_0 (W103). Once the width of the plate is sufficient to limit the yielding of the material in front of the bolt hole, the resistance no longer increases. The discrepancy in resistance between the predicted resistance and the experimental results is explained in detail in [13].

For single bolt connections, the Eurocode's linear model (Eqs. (4) – (6)) predicts stiffness well in the initial range up to a bearing stress of about 1.5 f_u. At higher bearing stresses, the linear model gives lower bolt hole elongations than in the experiments. The linear prediction in Fig. 9 is shown for M101 and M105 with M24 bolt ($k_d = 0.825$). M110 had smaller diameter bolt M16, which leads to lower stiffness ($k_d = 0.8375$). Since, the difference in stiffness is small, only the linear prediction for M101 and M105 is shown. In case of connections with large end distance shown in Figs. 13 and 14, the stiffness of the linear model is more a tangent stiffness while for other connections it is more a secant stiffness.

4.2. Connections with more bolts

Figs. 15 to 20 show the linear and non-linear predictions and experimental load-deformation curves for lap connections with 3, 4 and 5 bolts in double shear with different geometry, steel grades and failure modes. Detailed information on the connections can be found in [14,18,19], while the information required for the determination of the analytical load-deformation curves can be found in Table 4. In all cases presented, no significant shear deformations of the high-strength bolts were observed. Therefore, the bolts are assumed to be rigid. The prediction curves were generated assuming that the elongations of the bolt holes are equal. Since the elongation of the bolt hole due to the bearing action is much larger than the elastic deformation of the plate between the bolt holes, this assumption is justified. These assumptions greatly simplify the construction of the prediction curves since the bearing at the bolt holes is the only component. The relationship between load and deformation is established for each bolt hole, as shown in Fig. 8. Since the distances between the bolt holes are the same, only the relationship for the end and inner bolt needs to be constructed. The predicted response of the connection is obtained by summing the responses of the end and inner bolt holes. For connections with lap plates that are thicker than the inner plate, i.e. where the elongation of the bolt holes in the lap plate is insignificant, one end bolt hole and (n – 1) inner bolt holes are assumed, where n is the number of bolts in a connection. The lap plates of connections M405 and M508 had the same thickness (2 ×8 mm) as the inner plate (16 mm). In these cases, 2 end bolt hole and (n – 2) inner bolts holes are assumed, because the deformation of the lap plates was similar to the deformation of the inner plate.

The test curves in [14,18,19] were obtained by measuring the relative displacement between the lap and the inner plate. The measurement includes the elastic and plastic deformation of the plates. As mentioned earlier, the elastic deformation is insignificant. In cases where the failure mode is related to failure due to bearing action (tear-out of the end bolt, shear failure between bolt holes), the prediction curves can describe the response up to the maximum resistance. In cases where failure of the net cross-section or plastic deformation of the net cross-section has been observed, the prediction curves can only be compared to the test curves up to the point of where the net cross-section starts to yield. After the net cross-section yields, the deformation of the connection is concentrated in the net section and the resistance increases due to the material

Table 3
Data on single bolt connections.

Specimen	e_1/d_0	e_2/d_0	d_0 [mm	t [mm]	Bolt	f_u [MPa]	Failure mode
M101	1.23	1.23	26	12	M24	425	Shear/Splitting
M105	1.23	1.50	26	12	M24	425	Shear
M110	1.22	1.50	18	12	M16	425	Shear
B103	1.50	1.15	30	10	M27	885	Splitting
B111	1.51	1.48	30	10	M27	885	Splitting
B116	1.50	1.42	30	10	M27	885	Splitting
B117	1.50	1.48	30	10	M27	885	Splitting
B118	1.53	1.90	30	10	M27	885	Shear
B120	2.56	1.96	30	10	M27	885	Splitting
B121	3.06	2.06	30	10	M27	885	Splitting/Net cross-section
W101	3.03	2.43	30	10	M27	447	Shear fracture at end bolt
W102	3.00	3.07	30	10	M27	447	Shear fracture at end bolt
W103	2.99	4.03	30	10	M27	447	Shear fracture at end bolt
W104	3.01	5.01	30	10	M27	447	Shear fracture at end bolt
W105	3.49	5.01	30	10	M27	447	Shear fracture at end bolt
W106	3.83	7.52	30	10	M27	447	Shear fracture at end bolt
W107	4.44	7.51	30	10	M27	447	Shear fracture at end bolt
W108	5.04	3.36	30	10	M27	447	Shear fracture at end bolt
W109	5.00	5.03	30	10	M27	447	Shear fracture at end bolt
W110	4.94	7.47	30	10	M27	447	Shear fracture at end bolt
SD-20-30-550	2.00	3.00	26	10	M24	757	Shear
SD-20-30-690	2.00	3.00	26	10	M24	859	Shear
SD-20-30-890	2.00	3.00	26	10	M24	1064	Shear

hardening. The measured relative displacement between the lap and the inner plate of the connections M405 and M508 is due to the deformation of all plates. It is assumed that the deformation of the lap and the inner plates is equal. Therefore, the measured displacement of these connection was divided by two to obtain only the deformation of a single plate.

Two- and three-bolt HSS connections L03, TT-30–45-20-xxx and ThT-30–45-20-xxx (xxx stands for steel grade Q550D, Q690D or Q890D) with the same relative geometry (see Table 4) failed due to shearing of the plate between the bolt holes caused by high bearing forces. The response curves are shown in Figs. 15 and 16. Fig. 16b also shows specimen L03 after failure, while the photos of TT-30–45-20-xxx and ThT-30–45-20-xxx can be seen in [14]. It can be seen that the prediction curves describe the embedment phase well in all cases. For the connections with two bolts it accurately predicts the response up to the maximum resistance (in terms of engineering accuracy), while the prediction curve for connections with 3 bolts enters the plastic phase too early. The prediction curves for 3-bolt L03 and ThT-30–45-20-xxx connection are the same because the relative geometries are the same and the lap plates of all connections are stiffer than the inner plate.

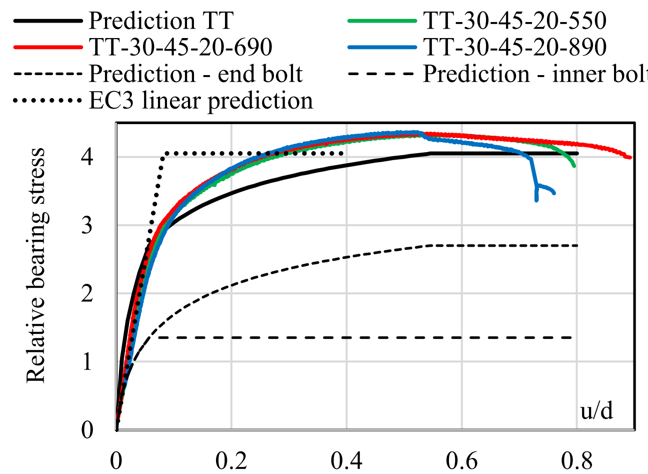

Fig. 15. Comparison of test result and predicted load-displacement curve for HSS connections with 2 bolts (see [14]).

Figs. 12, 15 and 16 clearly show that no particular conclusions can be drawn about the ductility of various HSS.

Figs. 17 and 18 show connections that have failed by tear-out of the first bolt. The prediction curve in the case of high strength (L14, steel S690) and mild steel (M405, steel S235) fits the test curve well. The factor k_m effectively reduces the resistance of the HSS connection L14 and makes it possible to determine the bearing resistance of the connection by summing the individual bearing resistances at the bolt holes. The M405 mild steel connection is characterized by an increasing slope of the response curve in the plastic phase, which is well predicted. In Fig. 18 can be seen that at the same time as the bolt tears-out, the net cross-section also yields completely, as a certain plastic deformation of the net cross-section can be observed.

Specimens L18 (steel S690) and M505 (steel S235) shown in Fig. 19 and Fig. 20 failed in the net cross-section. The connection deformed due to bearing at bolt holes until the net cross section yielded, which can be estimated as $F_y = A_{net} f_y$. Thereafter, the deformations developed mainly in the net cross-section, leading to necking and finally fracture. Therefore, the prediction curves can only be predicted up to the yielding of the net cross-section ($A_{net} f_y$). Predicting the behaviour beyond yielding of the net cross-section would require an analytical relationship of the hardening of the net cross-section. Fig. 19b shows the visible bolt hole elongations due to the bearing force, which are related to the high bearing resistance and the significant non-linear behaviour before the yielding of the net cross-section, which can be clearly seen in Fig. 19a. Since HSS S690 is characterized by a low ratio of ultimate to yield strength of 1.05, the ultimate resistance is not much greater than F_y. On the contrary, in Fig. 20b, there is hardly any noticeable elongation of the bolt holes. Although the bearing resistances at the bolt holes are low (clearly in the steep part of the embedment curve), the net cross-section yields. The S235 steel has the ability of significant strain hardening, which can also be observed in the test curve of M505 shown in Fig. 20a. The prediction curve agrees perfectly with the numerical simulation of M508 (curve M508 – FEA), while the differences with the test curve can be observed due to the initial slip and geometric imperfections (non-simultaneous formation of the contact between plate and bolt).

Similar to single bolt connections, the Eurocode's linear model (Eqs. (4)–(6)) predicts stiffness well in the initial range, i.e. when the utilization in bearing is low (see Fig. 20). Therefore, the linear model can be used to estimate the stiffness associated to serviceability condition, while the non-linear model more accurately estimates the decrease in stiffness associated with higher bearing stresses.

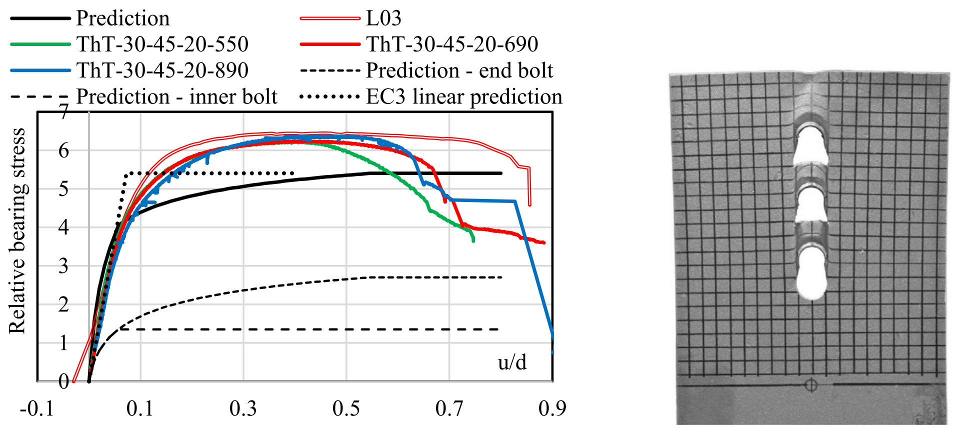

a) Connections with three bolts b) L03 after failure

Fig. 16. Comparison of test result, FEA and predicted load-displacement curve for HSS connections with 3 bolts, L03 see [18], ThT-30–45-20-xxx see [14].

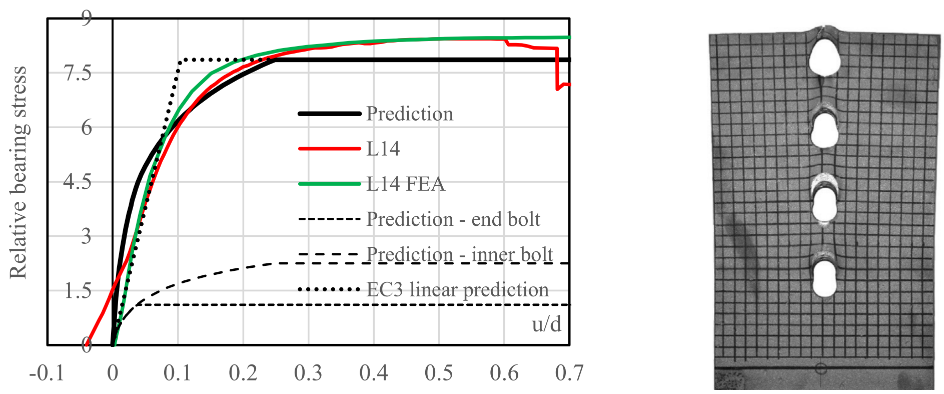

a) Response curves b) L14 after failure

Fig. 17. Comparison of test result, FEA (see [18]) and predicted load-displacement curve for specimen L14.

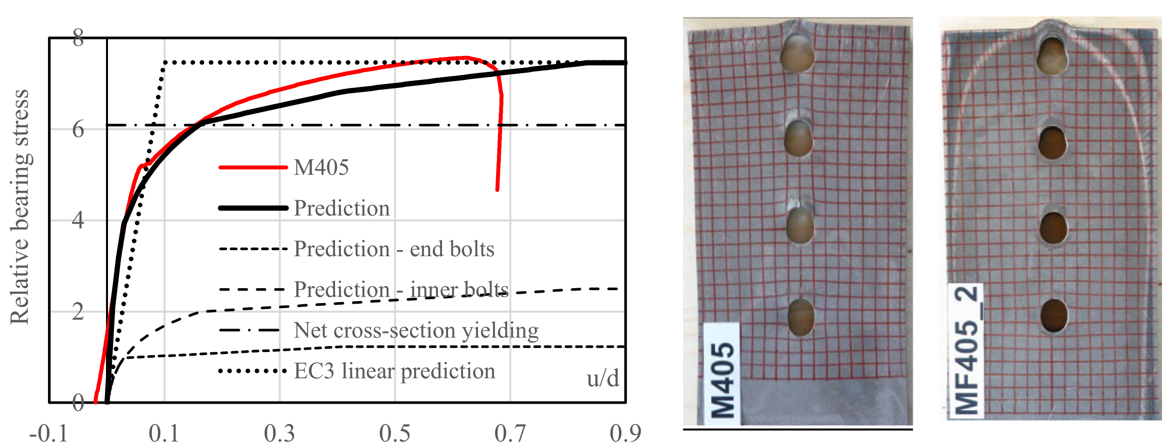

a) Load-deformation curves b) Inner plate c) Lap plate

Fig. 18. Comparison of test result (see [19]) and predicted load-displacement curve for specimen M405, [19].

4.3. Comparison of Eurocode load-deformation model for bearing

As mentioned above, the new Eurocode offers two load-deformation models for bearing. The linear model is given by Eqs. (4)–(6), while the non-linear model is described by Eqs. (7)-(10). A comparison between these two models for specific connections has already been shown. In this section, the linear model is compared relatively with the non-linear model. Therefore, the linear model must be expressed in a relative (non-dimensional) form. Let us start with a linear relationship for the bearing, which is as follows:

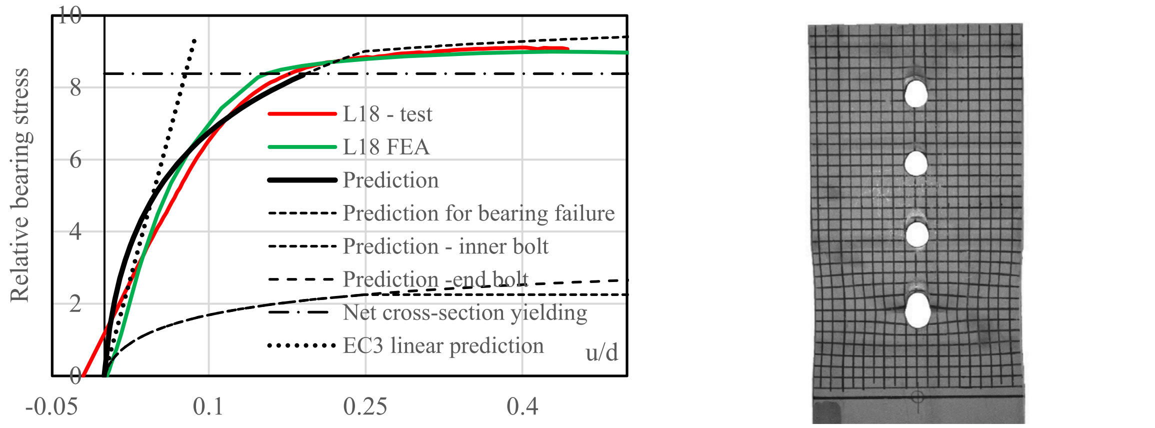

a) Response curves b) L18 just after maximum resistance

Fig. 19. Comparison of test result, FEA (see [18]) and predicted load-displacement curve for specimen L18.

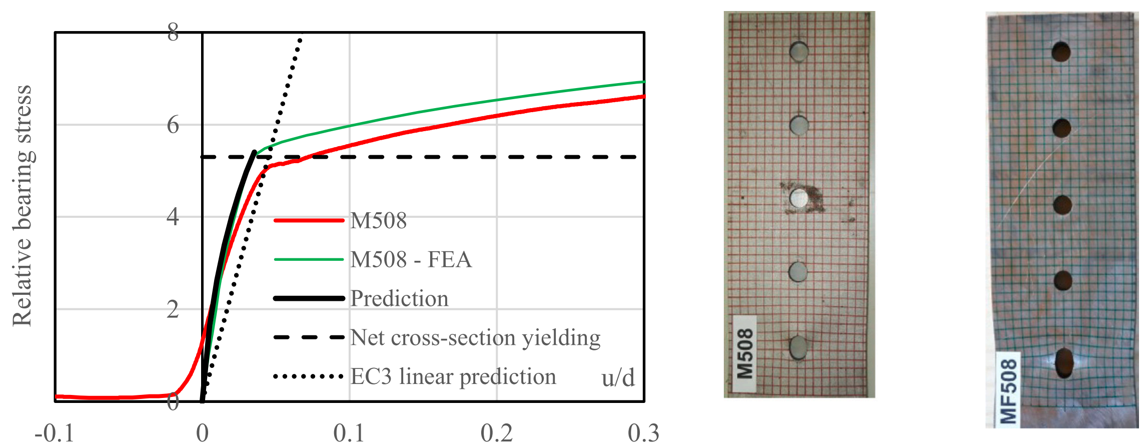

a) Load-deformation curves b) Inner plate c) Lap plate

Fig. 20. Comparison of test result, FEA (see [19]) and predicted load-displacement curve for specimen M508.

Table 4
Data on connections with several bolts.

Specimen	e_1/d_0	p_1/d_0	e_2/d_0	d_0 [mm]	t_1 [mm]	Σt_2 [mm]	No. bolts	Bolt	f_u [MPa]	Failure mode
L03	3	2	4.5	22	10	40	3	M20	844	P.S.
L14	1.23	3	4.5	22	10	40	4	M20	844	T.O.
L18	3	3	4.5	22	10	40	4	M20	844	N.S.
M405	1.23	3	3.86	22	16	16	4	M20	399	T.O.
M508	2	4	3.86	22	16	16	5	M20	399	N.S.
TT-30-45-20-550	3	2	4.5	26	10	20	2	M24	757	P.S.
TT-30-45-20-690	3	2	4.5	26	10	20	2	M24	859	P.S.
TT-30-45-20-890	3	2	4.5	26	10	20	2	M24	1064	P.S.
ThT-30-45-20-550	3	2	4.5	26	10	20	3	M24	757	P.S.
ThT-30-45-20-690	3	2	4.5	26	10	20	3	M24	859	P.S.
ThT-30-45-20-880	3	2	4.5	26	10	20	3	M24	1064	P.S.

$t_1$thickness of the inner plate
Σt_2sum of thicknesses of both lap plates
P.S.plate shear failure between bolt holes
T.O.tear-out of the first bolt
N.S.net cross-section failure

$$F_b = k_b\, u \tag{12}$$

F_b is the bearing force, k_b is the stiffness and u is the bolt hole elongation. Since this is a bi-linear relationship with a plastic plateau, only a single point is required to design the load-deformation curve. The plastic plateau starts when the maximum bearing resistance is reached. The bearing force F_b at this stage is given by Eq. (1). With this knowledge, the elastic bolt hole elongation u_{el} can be determined. A relative

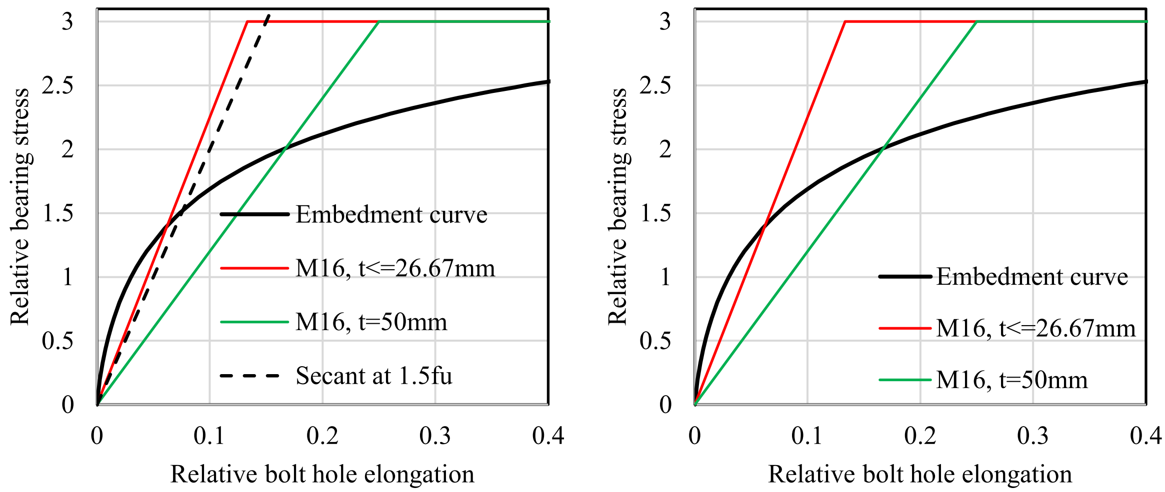

a) effect of bolt size b) effect of thickness

Fig. 21. Comparison of Eurocode load-deformation models for bearing for bearing resistance of 3 f_u.

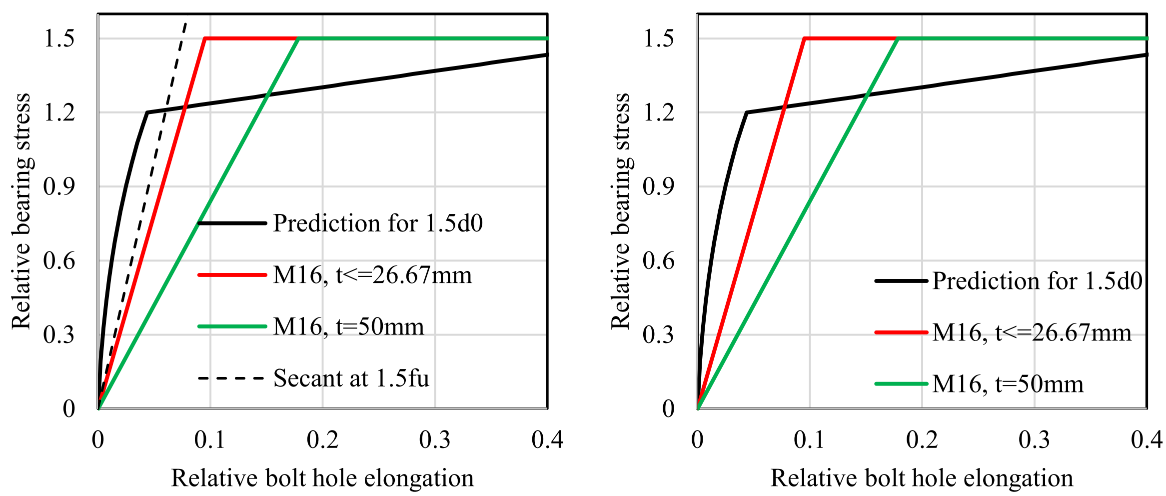

a) effect of bolt size b) effect of thickness

Fig. 22. Comparison of Eurocode load-deformation models for bearing for mild steel and bearing resistance of 1.5 f_u.

(non-dimensional) representation of the relationship is obtained by introducing Eqs. (1), (4) and (6) to Eq. (12). The relative elastic bolt hole elongation ($\overline{u}_{el}$), i.e. at the end of the linear part, is obtained after a simple derivation:

$$k_m\alpha_b = 18\,k_d\,\min\left(1;\ \frac{26.67\text{mm}}{t[\text{mm}]}\right)\frac{u_{el}}{d_{M16}}\cdot\frac{d}{d} = 18\,k_d\,\min\left(1;\ \frac{26.67\text{mm}}{t[\text{mm}]}\right)\frac{d}{d_{M16}}\overline{u}_{el} \tag{13}$$

$$\overline{u}_{el} = \frac{k_m\alpha_b}{18\,k_d}\cdot\frac{d_{M16}}{d}\cdot\max\left(1;\ \frac{t[\text{mm}]}{26.67\text{mm}}\right). \tag{14}$$

In contrast to the non-linear model which, when presented in non-dimensional form, is independent of tensile strength, bolt diameter and plate thickness. The linear model shows a dependance on bolt diameter and plate thickness. The comparison between the models is shown in Figs. 21 and 22, where for simplicity and ease of presentation it is assumed that the bolt diameter is equal to the bolt hole diameter ($d = d_0$). Fig. 21 shows the analytical load-deformation curves for bearing where maximum bearing stress is 3 f_u ($e_1 \geq 3d_0$ or $p_1 \geq 3.5d_0$). Fig. 21a shows that the stiffness of the linear model increases with the increase of the bolt diameter. The effect of the plate thickness is shown in Fig. 21b. The linear curve is the same for thicknesses below 26.67 mm. For greater thicknesses, the linear curve becomes less steep, which does not seem logical at first sight. The coefficient k_t given in Eq. (6) has a maximum limit of 2.5 when the plate thickness exceeds 26.67 mm, which limits the stiffness to an upper value when the calculation is done by units. Converting the non-dimensional form to the form with units requires multiplication by the thickness. To obtain a constant stiffness of the form with units, the slope of the curve must decrease with the increase of the thickness. The results in Fig. 22, showing the analytical load-deformation curves for bearing stress of 1.5 f_u ($e_1 \geq 1.5d_0$), are similar to the results in Fig. 21. In all cases, the linear model leads to secant stiffness, with better prediction for the cases with bearing forces of about 1.5 f_u.

It has already been shown that the load-deformation behaviour is independent of the plate thickness and the bolt diameter when represented in a non-dimensional form. The non-linear model for bearing

Table 5
Relative bearing resistance calculated at different bolt hole elongation.

Bolt	Relative bearing resistance $\overline{\sigma}_b$											
	M12		M14		M16	M20	M22	M24	M27	M30	M33	M36
Clearance Δ [mm]	**1**	**2**	**1**	**2**	**2**	**2**	**2**	**2**	**3**	**3**	**3**	**3**
Offset 0.5 Δ	1.2	1.6	1.1	1.5	1.4	1.3	1.2	1.2	1.3	1.3	1.2	1.2
Offset Δ	1.6	2.0	1.5	1.9	1.8	1.7	1.6	1.6	1.8	1.7	1.6	1.6
Offset 2 Δ	2.0	2.4	1.9	2.3	2.3	2.1	2.1	2.0	2.2	2.1	2.1	2.0

takes this assumption into account, while the linear model introduces several factors to account for the effects of geometry. A new, simpler linear model can be developed using the embedment curve evaluated for a bearing stress of 1.5 f_u. Such a model represents a "good guess" for estimating stiffness in the context of serviceability, where the utilization in bearing is low. Therefore, the secant stiffness is determined as follows. First, the inverse of the embedment curve is derived:

$$\overline{u} = \left(\frac{\sqrt{30} + \sqrt{\frac{30}{\overline{\sigma}_b}}}{\frac{126}{\overline{\sigma}_b} - 30} \right)^2 \tag{15}$$

The relative bearing stiffness is the ratio between the relative bearing stress and the relative bolt hole elongation and is determined using Eq. (15):

$$S_b = \frac{1.5}{\overline{u}(\overline{\sigma}_b = 1.5)} \doteq 20 \tag{16}$$

Finally, the secant stiffness is calculated as follows:

$$k_{bs} = 20\, t\, f_u. \tag{17}$$

The linear model with secant stiffness based on the embedment curve is shown in Figs. 21a and 22a.

5. Conclusions

The paper presents an analytical model for predicting the load-deformation behaviour for bearing included in the new EN 1993–1-8:2021. The model has been calibrated on the basis of finite element analyses and its suitability has been tested on test results of single and multiple bolt connections of different steel grades, geometries and failure modes. The main advantage of this model is that it accurately describes the bolt embedment phase (nominal elastic phase), where the deformation behaviour is non-linear, and provides a clear transition to the plastic phase, associated with large deformations of the bolt hole.

The bolt hole elongations due to the bearing action are not of concern in the ultimate limit state (ULS). The extent of deformations of the joint due to the bearing failure in the ULS is comparable to other failure modes, such as block tearing or net cross-section failure. However, the deformation of a joint in the ULS can become a problem, e.g. when stability is at stake (lap joint at mid height of a column). The load-deformation behaviour for bearing is characterized by significant local yielding of the material, where a small increase in bearing resistance leads to a large increase in deformation. Therefore, the bolt hole elongation should be controlled at the serviceability limit state (SLS) to prevent excessive yielding. A suitable limit value for the bearing resistance to prevent excessive yielding is defined as follows based on the presented behaviour:

$$F_{\mathrm{b,red}} = k_{\mathrm{m}} \alpha_{\mathrm{b,red}}\, d\ \ t\, f_u \tag{18}$$

$$\alpha_{\mathrm{b,red}} = \begin{cases} \min(\alpha_b;\quad 2) \text{ for steel grades} \geq \text{S460} \\ \quad \min(\ 0.8\ \alpha_b;\quad 2) \text{ otherwise} \end{cases} \tag{19}$$

where α_{b} is obtained from Eq. (2). The minimum of two values is suggested in the above equation, where the first particle (α_{b} or 0.8 α_{b}) is associated with end of the nominally elastic behaviour for small e_1 or p_1. However, this reduction leads in most cases to a limitation of the bearing stress of 2 f_{u}, where the bolt hole elongation of about $d/6$ is to be expected (see Eq. (9)). Considering the ratio between the combinations of actions in ULS and SLS, which is usually about 1.4 (max ($\alpha_{\mathrm{b,red}}$ / α_{b} = 1.5), and the fact that the bearing failure is rarely decisive in the design (usually the net cross-section failure, block tearing or shear failure of the bolt is decisive, where the bearing forces are relatively low), the limitation of the bearing resistance in SLS would not determine the design in vast majority of cases. Of course, the model presented can also be used to define other limits for controlling the bearing deformation.

The model can be easily applied in several cases, e.g. to estimate the deformation of a member due to the deformations of the joints, to derive the ductility criteria for nominally pinned joints with fin plates and to avoid premature bolt fracture for bolts in geometrically imperfect joints, which can be crucial for joints made of high-strength steels. All joints are geometrically imperfect due to the fabrication tolerances and bolts in clearance holes. The bolt holes are accidentally misaligned so that the bearing contacts do not occur simultaneously. According to Kulak et. al (page 93, [3]), the average hole offset is less than 0.8 mm. The load is distributed to all bolts after all bearing contacts are made. The elongation of the bolt holes and shear deformation of the bolt allows all bearing contacts to be formed and requires the bolts to resist the bearing forces. For the purpose of this demonstration, the shear deformation of the bolts is neglected. The problem can occur when the initial position of the bolt holes is most unfavourable. The worst case scenario [2] is when all bolts fit into the bolt holes while one or more bolt holes are displaced by two hole clearances in the direction of the force. The strength of the bolts is always sufficient if the ductility criterion is fulfilled, i.e. the design shear resistance of the bolt is larger than the design bearing resistance. If the ductility criterion is not fulfilled ("weak" bolts situation), a bolt or a group of bolts can fail before the force is distributed to all bolts, although

Table 6
Estimated maximum thickness of plates in lap joints with "weak" bolts in double shear, with the shear plane passing through the threaded part of the bolt – for an offset of 2 Δ.

Grades		Bolt size											
Steel	**Bolt**	**M12**		**M14**		**M16**	**M20**	**M22**	**M24**	**M27**	**M30**	**M33**	**M36**
S235	**8.8**	10	8	12	10	12	16	18	20	21	24	28	31
	10.9	10	9	12	10	13	17	19	21	22	25	29	32
S355	**8.8**	7	6	9	7	9	12	14	15	16	18	21	23
	10.9	8	6	9	8	9	12	14	15	16	19	21	24
S690	**8.8**	5	4	6	5	6	8	9	10	10	12	13	15
	10.9	5	4	6	5	6	8	9	10	11	12	14	15

Table 7
Estimated maximum thickness of plates in joints with "weak" bolts in double shear, with the shear plane passing through the non-threaded part of the bolt– for an offset of 2 Δ.

Grades		Bolt size											
Steel	**Bolt**	**M12**		**M14**		**M16**	**M20**	**M22**	**M24**	**M27**	**M30**	**M33**	**M36**
S235	**8.8**	13	11	16	13	15	20	23	26	26	30	34	38
	10.9	16	13	20	16	19	25	28	32	33	38	42	47
S355	**8.8**	10	8	12	10	11	15	17	19	20	22	25	28
	10.9	12	10	15	12	14	19	21	24	24	28	31	35
S690	**8.8**	6	5	8	6	7	10	11	12	13	14	16	18
	10.9	8	7	9	8	9	12	14	15	16	18	20	22

all design requirements in the ultimate limit state are fulfilled. The embedment curve (9) can be used to calculate the bearing resistance required to elongate the bolt hole for a given displacement required to overcome the initial offset. These values are given in Table 5 for offsets of 0.5, 1 and 2 times the bolt hole clearance Δ. It can be seen that bolts should be able to resist a relative bearing stress of about 1.2 for an offset of 0.5 Δ and a relative bearing stress of about 2 for an offset of 2 Δ. The greatest requirements apply to M16 bolt and M12 bolt in holes with 2 mm clearance. Normal round holes for M12 and M14 bolts have clearance of 1 mm [20], but 2 mm clearance is also permissible. The maximum thickness of plates in lap joints with "weak" bolts in double shear can be calculated from:

$$m\,F_{v,Rd} \geq \frac{\overline{\sigma}_b \cdot d \cdot t \cdot f_u}{\gamma_{M2}}, \tag{20}$$

where $F_{v,Rd}$ is the design shear resistance of the bolt and m is the number of shear planes. The equation is not affected by the partial factor as it also appears in $F_{v,Rd}$. Tables 6 and 7 show the maximum thickness of plates in lap joints with "weak" bolts in double shear, where the shear plane passes through the threaded and unthreaded parts of the bolt. The bolt hole offset of 2 Δ was considered in the calculation of values in the tables. It can be observed that the maximum plate thicknesses are limited to relatively thin plates, especially when HSS is used. Although it was assumed that the bolts do not deform in shear, the bolts have some ductility in shear. However, the available ductility is required to achieve the ultimate strength specified in the design rules for the case of "weak bolts". Therefore, the values in the table are rather a conservative assumption and further investigations are needed to obtain more realistic values. Similar tables are obtained in the case where the ductility criterion is fulfilled, where the restrictions are even more severe. The tests of geometrically imperfect lap connections from the literature [14, 18] show that insufficient strength of bolts can lead to premature bolt failure, i.e. before the force is distributed to all bolts. The tests in the literature were carried out with grade 12.9 bolts, which were strong enough, but the load-displacement curves clearly show that the bolts of lower grade would fail. In future work, the analytical model for bearing presented herein will be used to evaluate the effects of the non-linear distribution of bearing forces between bolts and the geometric imperfections in lap connections of steels with yield strength up to 1000 MPa.

Declaration of Competing Interest

The authors declare that they have no known competing financial interests or personal relationships that could have appeared to influence the work reported in this paper.

Acknowledgments

The research was carried out with financial support from the Slovenian Research and Innovation Agency under projects P2–0158 and N2–315. The authors sincerely thank Dr. Yan-Bo Wang and his colleagues for making their research results available.

References

[1] Fisher JW, Rumpf JL. Analysis of bolted butt joints. J Struct Div 1965;91:181–204.
[2] Henriques J, Jaspart JP, da Silva LS. Ductility requirements for the design of bolted lap shear connections in bearing. Adv Steel Constr 2014;10:33–52.
[3] G.L. Kulak, J.W. Fisher, J.H.A. Struik, Guide to Design Criteria for Bolted andRiveted Joints, 2nd ed., American Institute Of Steel Construction, Inc., Chicago, 2001.
[4] CEN, Eurocode 3: Des Steel Struct — Part 1-8: Jt, FprEN 1993-1-8, CEN/TC 250/SC 3 N 3743 2023 214.
[5] C.E.N., Eurocode 3: Design of steel structures - Part 1–8: Design of joints, EN 1993–1-8, Belgium. (2005).
[6] Može P, Yang F, Veljkovic M. Validation and application of bearing and block tearing resistance; background to prEN1993-1-8:2021. J Constr Steel Res 2021; 187:106985. https://doi.org/10.1016/J.JCSR.2021.106985.
[7] Latour M, Rizzano G. Numerical study on the resistance of thread-fixed one-side bolts: Tensile and bearing strength. Structures 2021;32:958–72. https://doi.org/10.1016/J.ISTRUC.2021.03.083.
[8] C.O. Rex, W.S. Easterling, Behavior and modeling of a bolt bearing on a single plate, J. Struct. Eng. 129 (2003) 792–800. https://doi.org/Doi 10.1061/(Asce)0733–9445(2003)129:6(792).
[9] Može P, Beg D. A complete study of bearing stress in single bolt connections. J Constr Steel Res 2014;95. https://doi.org/10.1016/j.jcsr.2013.12.002.
[10] P. Može, Deformation capacity, stiffness and bearing strength at bolt holes, in: 8th Int. Work. Connect. Steel Struct., AISC, Boston, USA, 2016.
[11] Lyu Y-F, Li G-Q, Wang Y-B. Behavior-based resistance model for bearing-type connection in high-strength steels. J Struct Eng 2020;146:04020109. https://doi.org/10.1061/(ASCE)ST.1943-541X.0002639.
[12] A. Ahmed L.H. Teh Thread Eff stiffness bolted Shear Connect 2019 doi: 10.1016/j.jcsr.2019.05.023.
[13] Može P. Bearing strength at bolt holes in connections with large end distance and bolt pitch. J Constr Steel Res 2018;147. https://doi.org/10.1016/j.jcsr.2018.04.006.
[14] Lyu YF, Li GQ, Wang YB, Li H, Wang YZ. Bearing behavior of multi-bolt high strength steel connections. Eng Struct 2020;212:110510. https://doi.org/10.1016/j.engstruct.2020.110510.
[15] Toussaint E, Durif S, Bouchaïr A, Grédiac M. Strain measurements and analyses around the bolt holes of structural steel plate connections using full-field measurements. Eng Struct 2017;131:148–62. https://doi.org/10.1016/J.ENGSTRUCT.2016.11.033.
[16] Može P, Beg D. High strength steel tension splices with one or two bolts. J Constr Steel Res 2010;66. https://doi.org/10.1016/j.jcsr.2010.03.009.
[17] Wang YB, Lyu YF, Li GQ, Liew JYR. Behavior of single bolt bearing on high strength steel plate. J Constr Steel Res 2017;137:19–30. https://doi.org/10.1016/j.jcsr.2017.06.001.
[18] Može P, Beg D. Investigation of high strength steel connections with several bolts in double shear. J Constr Steel Res 2011;67:333–47.
[19] P. Može, D. Beg, Bearing resistance of bolted connections, Nord. Steel Constr. Conf. (2012) 645–654.
[20] CEN, Execution of steel structures and aluminium structures - Part 2: Technical requirements for steel structures, EN 1090–2. (2018) 1–204.